# TURBULENT ENERGY AND DAMPING FUNCTIONS AT GAS-LIQUID INTERFACES AND WAVY WALLS

**Valerio De Angelis, Sanjoy Banerjee**
Department of Chemical Engineering,
University of California Santa Barbara
Santa Barbara (CA), 93106 USA
valerio@mindflash.com, banerjee@chemengr.ucsb.edu

## ABSTRACT

Reynolds averaged turbulence models require damping function models, e.g. those of Van Driest and Miner, to correctly describe the behavior of the various turbulence quantities of interest in Computational Fluid Dynamics (CFD). The behavior of such models when boundaries and boundary conditions are complicated is poorly understood. Direct Numerical Simulations (DNS) are presented here for two cases, viz. gas-liquid flow with a flat, horizontal interface (the high surface-tension limit) and gas flow over a wavy boundary. The DNS results are used to validate simple forms of the damping functions.

The Miner formulation of the damping function gives satisfactory results on the gas side, whereas the Van Driest formulation is more suitable on the liquid side for the case of turbulent gas and liquid streams coupled across a flat interface. In the case of flow over the wavy wall, Miner's model gives acceptable predictions for $\overline{u_1'u_3'}$ and $\overline{u_1'u_1'}$ but fails to predict $\overline{u_3'u_3'}$. The results are of some practical interest considering that these simple formulations of damping functions are routinely used in CFD codes to solve problems with complex geometries and boundary conditions.

## INTRODUCTION

Direct numerical simulation (DNS) may be used to develop and/or validate models of turbulence that are of practical use, such as subgrid-scale and Reynolds averaged models. Such models involve many assumptions and, in some cases, adjustable parameters that need to be "tuned" against experiments or DNS. The behavior of such practical models near boundaries of various sorts is of crucial importance. In fact most transport processes occur at boundaries, where these models are the weakest. We consider here two cases. The first case is DNS of a gas and liquid stream (with physical properties of an air-water system) flowing horizontally and counter-currently, coupled through a continuous interface (Lombardi *et al.*, 1996). The calculations are for a flat interface in the limit of very high surface tension. The boundary conditions at the interface are continuity of stress and velocity. This leads to differences in the behavior of the various terms in the kinetic energy transport equation on each side of the interface. The second case is DNS of a gas stream flowing over a rigid sinusoidal wavy wall (De Angelis *et al.*, 1997). The shape of the boundary introduces flow variations in the streamwise direction that effect turbulent quantities. Average turbulent quantities become, in fact, function of $x_1$, the streamwise coordinate. The steepness of the waves is low enough that the flow stays attached to the wall.

In the following sections we will use DNS data to estimate the parameters in various damping functions. We first define some important quantities. Equations 1 and 2 are the ensemble averaged momentum and continuity equations (average bars have been removed where no ambiguity can arise):

$$\nabla u_i = 0 \tag{1}$$

$$\frac{\partial u_i}{\partial t} + \frac{\partial \overline{u_i'u_j'}}{\partial x_j} = -\frac{\partial p}{\partial x_i} + \frac{1}{Re}\nabla^2 u_i \tag{2}$$

This system of equations could be used to compute **u** if a model for the Reynolds stress term, $\frac{\partial \overline{u_i'u_j'}}{\partial x_j}$, can be found. The simplest possible constitutive equation for the Reynolds stress is:

$$-\overline{u_i'u_j'} = 2\nu_t S_{ij} - \frac{2}{3}\delta_{ij}(\nu_t \frac{\partial u_k}{\partial x_k} + k) \tag{3}$$

Where $S_{ij}$ is the rate of strain tensor and $\nu_t$ is the turbulent viscosity, usually a function of the velocity field.

The quantity $\nu_t$ is usually written in the form:

$$\nu_t = c_\mu f_\mu \frac{k^2}{\epsilon} \tag{4}$$

in which $k$ and $\epsilon$ are the kinetic energy and dissipation rate and the quantities to model are $f_\mu$, the damping function, and the constant $c_\mu$. The function $f_\mu$ is also constant away from the boundaries. The role of $f_\mu$ is to account for the damping of the flow near the boundaries. In this study we use two different formulations of $f_\mu$. The two expressions used, $f_\mu^{VDR}$ and $f_\mu^{MIN}$, are due to Van Driest (1956) and Miner *et al.*(1991) and are chosen because of their simplicity and widespread use in the CFD community.

$$f_\mu^{VDR} = \left[1 - e^{-z^+/A^+}\right]^2 \tag{5}$$

$$f_\mu^{MIN} = f_0 + (1 - f_0) \cdot \left[1 - e^{-(z^+ - z_0^+)/A^+}\right]^2 \tag{6}$$

We can calculate $\nu_t$ and $f_\mu$ from the DNS results. We can then estimate the parameters in equations 5 and 6 and compute turbulence statistics a posteriori. The value of $c_\mu f_\mu$ is computed from DNS results as:

$$c_\mu f_\mu^{DNS} = \frac{-\epsilon - k_{,jj} - \nu_{t,j}k_{,j}}{k_{,jj} + (u_{1,j})^2} \tag{7}$$

Equation 7 is derived from the kinetic energy balance after averaging and using equations 3 and 4. The quantity $z^+$ is the distance from the boundary of interest measured in shear units. The simulations for the two cases presented here are done for a constant, fixed pressure drop-driven flow. For the case of gas flow over a flat interface, the macroscopic momentum balance gives $\Pi 2h = \tau$, where $\Pi$ is the macroscopic pressure drop in the streamwise direction and $\tau$ is the shear at the interface. The reference velocity, $u_\star$, is then given by $u_\star = \sqrt{2\Pi h/\rho}$ that coincides in this case with $u_\tau = \sqrt{\tau/\rho}$. The Reynolds number can be defined then as $Re = u_\star(\text{or } u_\tau)h/\nu$, where $\nu$ is the kinematics viscosity. In the case of flat gas-liquid interface then $z^+ = Rehx_3$, where $x_3$ is the non dimensional distance from the interface. For the case of flow over a wavy interface $u_\tau$ is smaller than $u_\star$ as some of the energy of the pressure drop goes into form drag. In this case the definition of $z^+$ is more complicated and postponed to a later section. In this manuscript $x_1$ and $x_3$ are used when talking about domain dimensions. Instead $z^+$ is used when describing turbulence quantities at different locations away from the boundary. Note again that for flow over flat gas-liquid interface is $z^+ = Rehx_3$.

## GAS-LIQUID INTERFACE

DNS results (Lombardi*et al.*, 1995) for high liquid to gas density ratio (~1000) show that in the near interface region the turbulence on the gas side has characteristics similar to that near the wall in channel flow turbulence, whereas on the liquid side fluctuations in the streamwise and spanwise directions are practically unimpeded at the interface and therefore the velocity field shares some of the characteristics of free-surface turbulence. This affects terms in the kinetic energy transport equation. Only the viscous diffusion term is similar on the two sides. On the liquid side the production term is more pronounced and the imbalance between production and dissipation rate is larger than on the gas side. The most remarkable difference is in the turbulent diffusion term which is positive at the interface ($z^+ = 0$) on the liquid side whereas it vanishes on the gas side (see Figure 1). Furthermore, the gas side shows a positive peak at $z^+ \sim 5$, whereas the liquid has its maximum positive value at the interface.

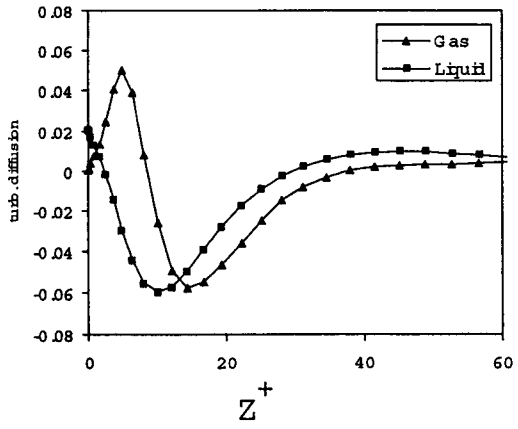


Figure 1: Comparison between the turbulent diffusion term on the gas and liquid sides. Note how the turbulent diffusion term peaks right at the interface on the liquid side.

Therefore we expect the form of the eddy viscosity and of the damping function, $f_\mu$, to be different on the gas and liquid sides of the interface. On the gas side the Miner model, $f_\mu^{MIN}$, in equation 6 fits the DNS data well. The values of the adjustable parameters are close to but somewhat different from those that give best agreement for turbulent flow over a flat wall (channel flow). This is to be expected since the gas sees the liquid like a solid boundary due to high liquid inertia. On the liquid side of the interface, however, the Van Driest's form of the damping function, $f_\mu^{VDR}$ (equation 5), needs to be used. The values of $f_\mu$ from the DNS and from the correlations (top), and the terms in the energy budget are shown in Figure 2 (gas side) and 3 (liquid side). Note that results are poor when, for example, $f_\mu^{MIN}$ is used on the liquid side or $f_\mu^{VDR}$ on the gas side. The values of the parameters in the damping functions $f_\mu^{MIN}$ and $f_\mu^{VDR}$ are reported in Table I

**Table I: Parameters in damping functions for gas-liquid flow**

| CASE | $C_\mu$ | $f_o$ | $z_o^+$ | $A^+$ |
|---|---|---|---|---|
| MIN - Channel | 0.17 | 0.027 | 7.08 | 32.7 |
| MIN - Gas | 0.12 | 0.042 | 6.69 | 26.03 |
| V-D - Liq | 0.086 | - | - | 31.1 |
| V-D - Literature | 0.09 | - | - | 26 |

## WAVY SOLID WALL

We examine now the case of gas flow over a no slip wavy (sinusoidal) boundary. Results for this case are discussed in details in De Angelis *et al.*(1997) The wavelength of the sine wave used here is similar to those of capillary waves. Therefore this case can elucidate some of the wave effects on gas side momentum transfer in a relatively simple situation. The case discussed here is for $\lambda/2h$=2.09 and a/$\lambda$=0.025 ($x_3 = a\sin\lambda x_1$). In Figure 4 the average streamlines over one period are shown. The flow stays attached to the boundary but the boundary layer thickness changes over the sine profile of the boundary.

We now briefly discuss some key features of turbulent quantities. In Figure 5 contour plots of the *r.m.s.* (root mean square) of the velocity fluctuation in the three directions are shown. Note that turbulence statistics vary along the direction of the flow, $x_1$. The velocity *r.m.s.* in Figure 5 are computed by considering fluctuations around the local average, $u_i' = u_i(x_1, x_2, x_3, t) - \overline{u(x_1, x_3)}$. In other words the velocity *r.m.s* vary in the $x_1$ and $x_3$ directions. The streamwise velocity *r.m.s.* value ($U_1^{r.m.s.}$) is above the average for regions above the wave troughs. The *r.m.s.* of the spanwise ($U_2^{r.m.s.}$) and vertical ($U_3^{r.m.s.}$) velocity fluctuations are above the average when the flow is going toward the crest of the wave.

The high value of $U_2^{r.m.s.}$ is limited to a very thin layer near the wall. The high value of $U_3^{r.m.s.}$ extends well above the wavy wall. In fact, it is known that on a concave surface there is a positive turbulent production term associated with the positive gradient of $u_3$ in the $x_1$ direction, *i.e.*the flow is accelerating, and this generates an increase in the turbulent intensities.

In here we discuss the capability of equation 6 of predicting the behavior of flows with a moderate boundary curvature like the one discussed here. Again the parameters in equation 6 are computed by fitting the damping function as computed from DNS results (equation 7). Once the parameters for equation 6 are computed, equation 3 can

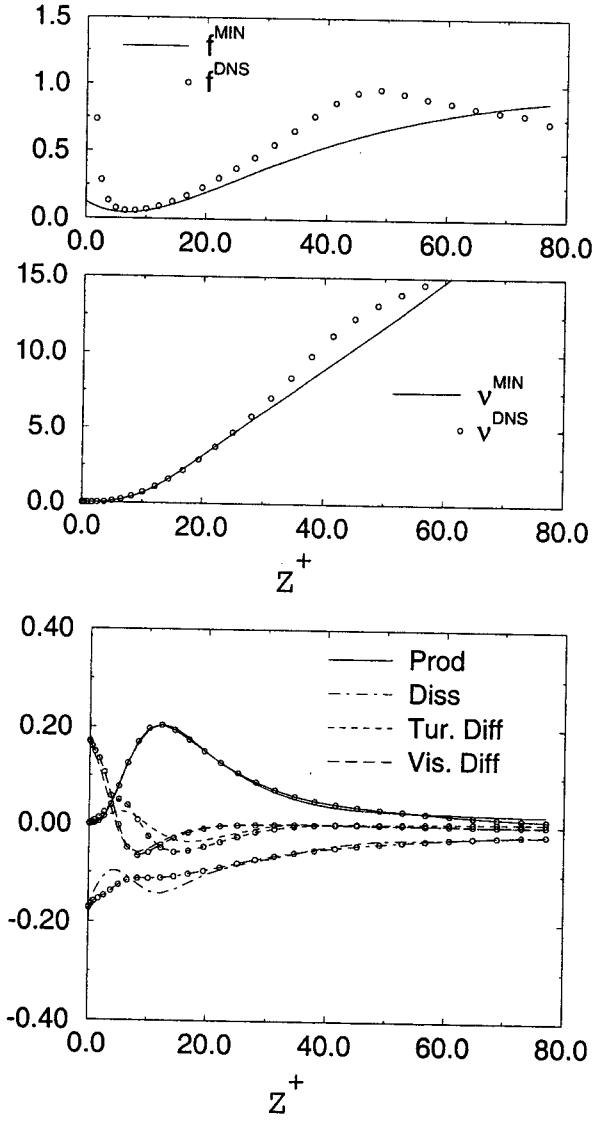


Figure 2: Gas side. Damping function (top) and eddy viscosity (middle). Terms in the energy budget (bottom). The symbols are DNS results. The lines are computed using the Miner model (1991) of equation 6 with the set of constants in Row 2 of Table I (MIN – Gas). The values in the ordinate are listed in the Figure labels.

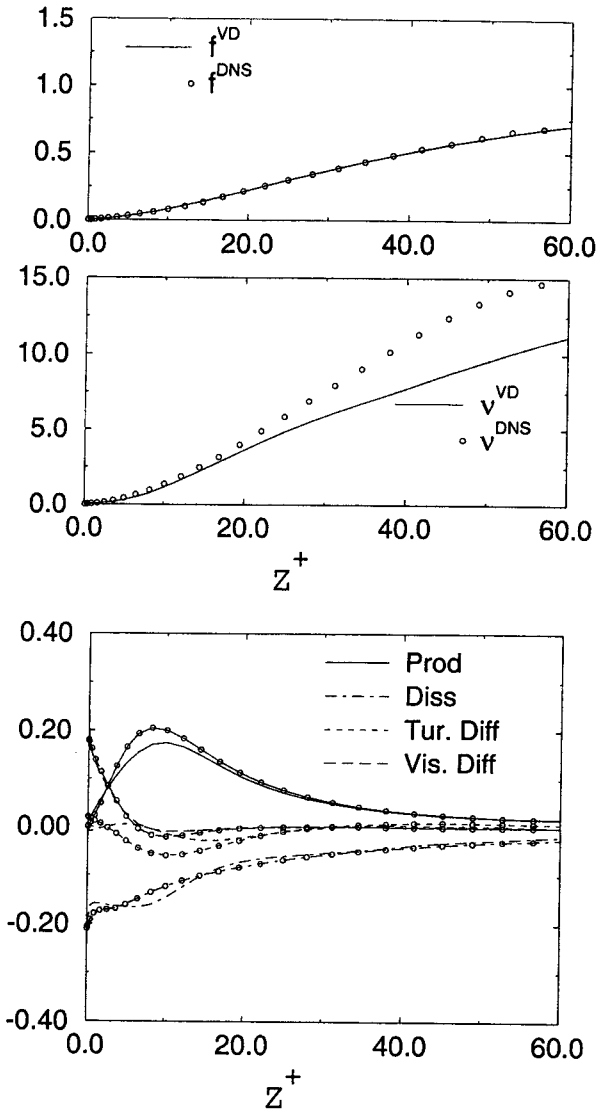


Figure 3: Liquid side. Damping function (top) and eddy viscosity (middle). Terms in the energy budget (bottom). The symbols are DNS results. The lines are computed using the Van Driest model (1956) of equation 5 with the set of constants in Row 3 of Table I (V-D – Liq). The values in the ordinate are listed in the Figure labels.

be used to compute the Reynolds stress terms a posteriori. Note that in this case the fit (in equation 7) is done using statistics that vary in the $x_1$ and $x_3$ directions. Before fitting the DNS data we rescale the non-dimensional velocity as:

$$z^+(x_1) = z_\star \cdot \mathrm{Max}\left(1, \frac{d\overline{u_1(x_1)}}{dx_3} \Big/ \frac{d\overline{\overline{u_1}}}{dx_3}\right) \qquad (8)$$

to account for the thinning and thickening of the streamlines. Note that $z_\star$ is based on $u_\star$ as defined in the introduction. The choice of $z^+$ is based on the fact that DNS results indicate that phenomena in the boundary layer scale well with the shear velocity (based on the average value of the shear stress at each $x_1$ position).

Figures 6-8 show the comparison of the Reynolds stress terms computed from equations 3 and 6 with those obtained from DNS results. In Table II we report the parameters obtained from the fit of the DNS data. Note that the values of the parameters are similar to those obtained for the case

Figure 4: Average Streamlines over one period. The flow stays attached to the boundary in the troughs of the wave profile. The complete domain contains 3 sine periods.

of flow over a flat wall.

The Reynolds stresses in the Figures are $\overline{u_1'^2}$, $\overline{u_3'^2}$ (the square of the *r.m.s.*) and $\overline{u_1' u_3'}$. Note again that these quantities vary in the $x_1$ and $x_3$ directions but the wall damping function in equations 6 depends explicitly only on the $z^+$ coordinate and that the dependency on $x_1$ is hidden in the definition of $z^+$ (equation 8).

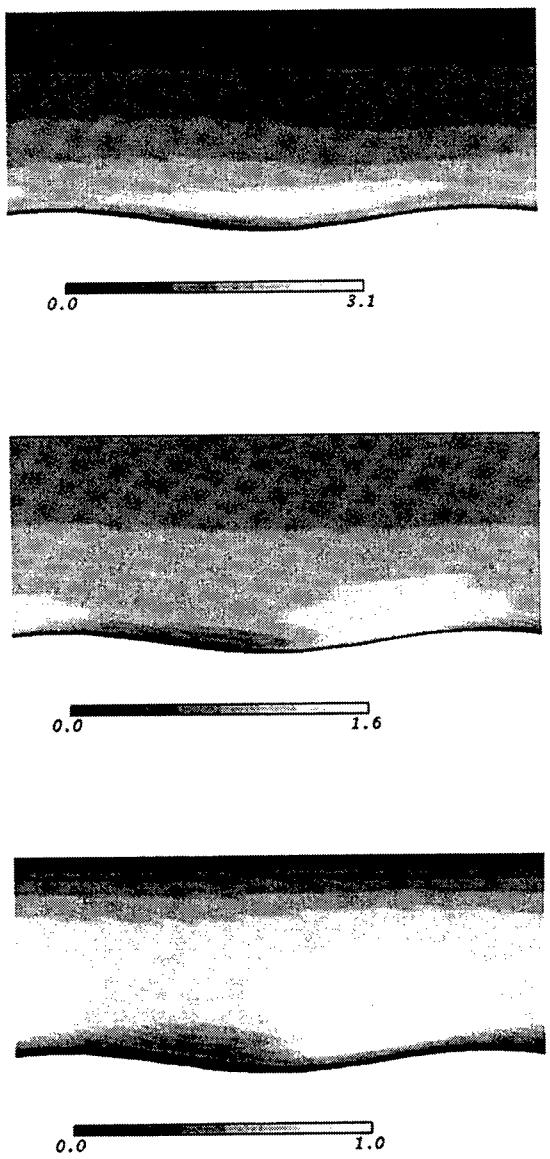


Figure 5: Root mean square fluctuations, reference velocity $\sqrt{2}u_*$. From top to bottom $r.m.s$ for $u_1$, $u_2$ and $u_3$.

**Table II: Parameters in damping function for the case of flow over a wavy wall.**

| CASE | $C_\mu$ | $f_o$ | $z_o^+$ | $A^+$ |
|---|---|---|---|---|
| MIN - Waves | 0.0981 | 0.1068 | 9.5527 | 27.4142 |

In Figure 6 we show the contours of $\overline{u_1' u_3'}$, for the DNS (Top) and the values computed from the model (Bottom). The agreement is satisfactory. The region of high $\overline{u_1' u_3'}$ is well predicted.

The agreement of $\overline{u_1'^2}$ with DNS data (Figure 7) is very good. The problem with the model appears, however, in the $\overline{u_3'^2}$ term (Figure 8). This terms is dominated by the $2/3\,k$ part of equation 3. The model predicts values of $\overline{u_3'^2}$ similar to those of $\overline{u_1'^2}$. In order to have better predictions for flows over curvilinear boundaries, more complicated models of the damping functions, which take anisotropy of the Reynolds stress into account, are required.

## CONCLUSION

It is clear that Reynolds averaged models and damping functions need to be selected carefully when boundary conditions and the domain geometries become complicated. In this manuscript we analyze the capabilities of simple damping functions of predicting turbulence quantities. DNS can help to decide how to select damping functions. A comparison of Table I and II shows that the constants for the three cases, channel flow, gas flow and flow over a wavy wall are in fact similar. In Figure 9 (top) we show the $\overline{u_1' u_3'}$ term for the case of flow over a wavy wall. The four curves are the DNS data and results computed using $f_\mu$ for the three combinations of parameters in Tables I and II (MIN - Channel, MIN - Gas, and MIN - Waves). It is clear how the values of the parameters for gas flow (MIN - Gas) gives acceptable results even for flow over wavy wall, making it the set of parameters that best matches the cases analyzed. This is clear from the bottom of the Figure in which the error, defined as $(\text{Value}_{DNS} - \text{Value}_{Model})^2/\text{Value}^2_{DNS}$, is shown for the three sets of parameters. On the liquid side only one case has been analyzed and the Van Driest model seems to give acceptable results.

In conclusion, we suggest use of the Miner model on the gas side with the set of constants in Row 2 of Table I (MIN - Gas), and on the liquid side we suggest the Van Driest model with the set of constants in Row 3 of Table I (V-D - Liq).

In future studies the case of gas-liquid flow over a deforming interface will be analyzed to expand the study and investigate the effect of mobile boundaries on the damping functions.

## REFERENCES

[1] P. Lombardi, V. De Angelis, and S. Banerjee. Direct numerical simulation of near-interface turbulence in coupled gas-liquid flow. *Physics of Fluid*, 8(6):1643–1665, 1996.

[2] E. W. Miner, T.S. Swean Jr., R.A. Handler, and R. Leighton. Examination of wall damping $k - \epsilon$ turbulence model using direct numerical simulations of turbulent channel flow. *Int. J. for Numerical Methods in fluids*, 12:609–624, 1991.

[3] E.R. Van Driest. On turbulent flow near a wall. *J. Aeronaut. Sci*, 23:1007–1011, 1956.

[4] De Angelis, V. and Lombardi, P. and Banerjee, S. , Direct numerical simulation of turbulent flow over a wavy wall, *Physics of Fluids*, 9(8): 2429–42, 1997.

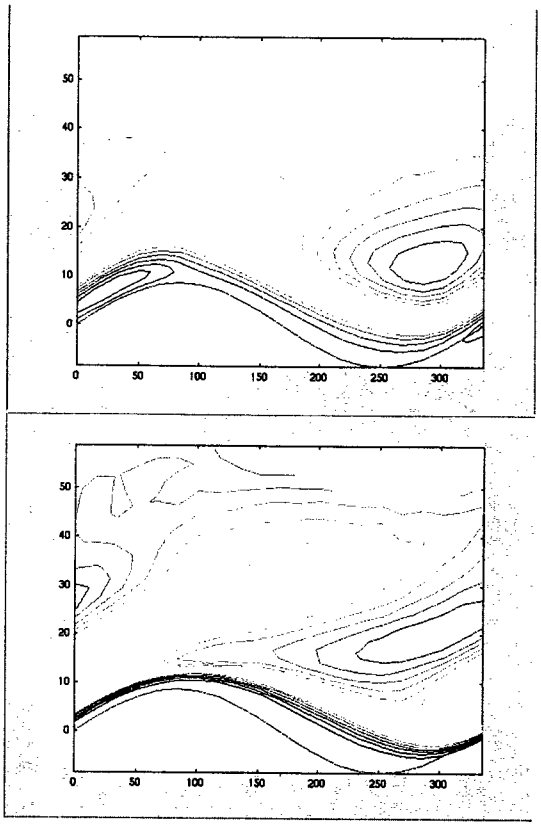

Figure 6: Results of Miner's model for $\overline{u_1' u_3'}$ over one wave period. On the top are the DNS results, on the bottom the prediction of the model. The coordinates are in shear units.

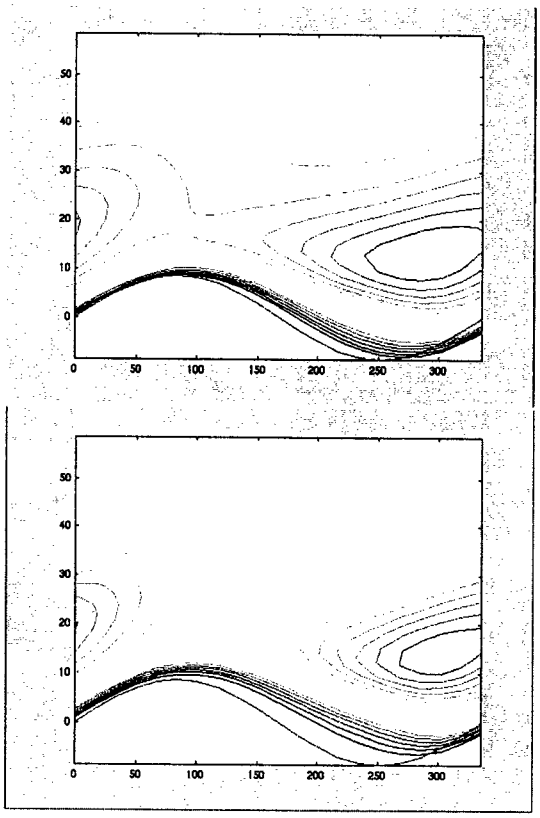

Figure 7: Results of Miner's model for $\overline{u_1'^2}$ over one wave period. On the top are the DNS results, on the bottom the prediction of the model. The coordinates are in shear units.

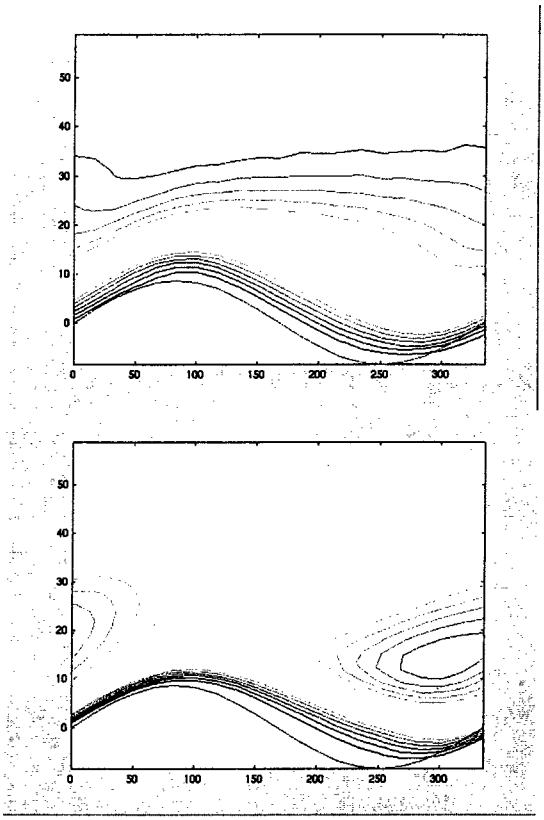

Figure 8: Results of Miner's model for $\overline{u_3'^2}$ over one wave period. On the top are the DNS results, on the bottom the prediction of the model. The coordinates are in shear units.

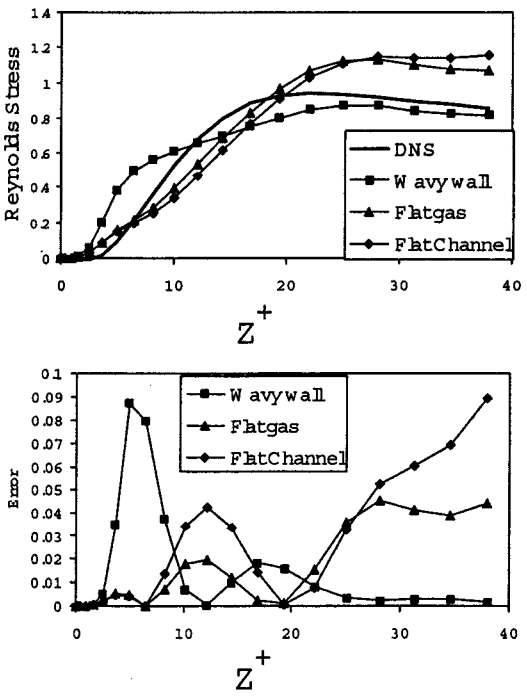


Figure 9: Results of Miner's model. Results for the average $\overline{u_1' u_3'}$ quantity in the case of flow over a wavy wall. The curves are computed using the parameters in Table I and II (MIN - Channel, MIN - Gas, and MIN - Waves).